Felix Nippert, Anna Nirschl, Tobias Schulz, Gordon Callsen, Ines Pietzonka, Steffen Westerkamp, Thomas Kure, Christian Nenstiel, Martin Strassburg, Martin Albrecht, Axel Hoffmann

# Polarization-induced confinement of continuous hole-states in highly pumped, industrial-grade, green InGaN quantum wells



JOURNAL OF APPLIED PHYSICS **119**, 215707 (2016)

# Polarization-induced confinement of continuous hole-states in highly pumped, industrial-grade, green InGaN quantum wells

Felix Nippert,[1,a)] Anna Nirschl,[2] Tobias Schulz,[3] Gordon Callsen,[1] Ines Pietzonka,[2] Steffen Westerkamp,[1] Thomas Kure,[1] Christian Nenstiel,[1] Martin Strassburg,[2] Martin Albrecht,[3] and Axel Hoffmann[1]
[1]*Institut für Festkörperphysik, Technische Universität Berlin, Hardenbergstraße 36, 10623 Berlin, Germany*
[2]*OSRAM Opto Semiconductors GmbH, Leibnizstraße 4, 93055 Regensburg, Germany*
[3]*Leibniz-Institut für Kristallzüchtung, Max-Born-Straße 2, 12489 Berlin, Germany*

(Received 30 March 2016; accepted 23 May 2016; published online 7 June 2016)

We investigate industrial-grade InGaN/GaN quantum wells (QWs) emitting in the green spectral region under high, resonant pumping conditions. Consequently, an ubiquitous high energy luminescence is observed that we assign to a polarization field Confined Hole Continuum (CHC). Our finding is supported by a unique combination of experimental techniques, including transmission electron microscopy, (time-resolved) photoluminescence under various excitation conditions, and electroluminescence, which confirm an extended out-of-plane localization of the CHC-states. The larger width of this localization volume surpasses the QW thickness, yielding enhanced non-radiative losses due to point defects and interfaces, whereas the energetic proximity to the bulk valence band states promotes carrier leakage. *Published by AIP Publishing.*
[http://dx.doi.org/10.1063/1.4953254]

## I. INTRODUCTION

InGaN/GaN quantum wells (QWs) are commonly applied in light emitting diodes (LEDs) and laser diodes (LDs) in the blue and even green spectral region.[1–3] However, both device types suffer from a distinct efficiency reduction towards the green spectral range, despite the better confinement properties of energetically deeper QWs. Established reasons for this matter include a reduced electron-hole-overlap in the QWs due to the quantum-confined Stark effect (QCSE)[4–8] and general difficulties in growing homogeneous InGaN material.[9–15] Also high pumping conditions are known to cause a further reduction of the efficiency that is attributed to Auger recombination.[16–19] In this letter, we report on an additional high excitation loss mechanism arising from confined hole continuum (CHC) states promoting carrier leakage, which is of utmost importance for the implementation of efficient LDs emitting in the green spectral region.

## II. METHODS

### A. Sample growth

A large quantity of high quality InGaN QW samples with different structural parameters was investigated in order to support the generality of the presented findings. The growth was conducted by means of metal-organic vapor phase epitaxy on c-plane sapphire substrates. The active region was deposited on a 3 $\mu$m thick GaN buffer and consists of five identical InGaN QWs separated by 27 nm thick GaN barriers. Such thick barriers reduce the influence of the individual QWs onto each other, which means that they can be treated as uncoupled single QWs ("quasi-SQW"). Subsequently, the active region was overgrown with an $Al_{0.15}Ga_{0.85}N$ electron blocking layer (25 nm) and a GaN capping layer (80 nm). The samples analyzed are nominally undoped, and the QWs have the nominal thicknesses between 2 nm and 3 nm and an Indium content of about 20%, resulting in emission wavelengths around 500 nm. Control samples with varying QW thicknesses (up to 4.3 nm), doping concentration in the barriers (up to $5 \times 10^{18}$ cm$^{-3}$ Si), and emission wavelengths (485–570 nm) were grown in order to verify that the observed effects do not depend on the magnitude of the QCSE, a lack of free carriers, or any general QW property like thickness or composition. While all presented observations are valid for all of these samples, a particular set of samples was chosen exhibiting a weak QCSE-caused shift with excitation power density.[5,7,8] This choice eases an understanding of the reported phenomena, as none of the observations need to be uncoupled from additional dynamic processes imposed by the (de-)screening of the QCSE. In addition, a complete multi quantum well (MQW)-LED structure with n- and p-doped layers and commercial-grade QWs of similar thickness and composition was investigated. Consequently, the application of a DC bias to the sample becomes feasible in order to approve carrier localization. All samples represent the state-of-the-art in InGaN QW growth, with growth parameters kept to values as similar as possible to industrial mass production and are the brightest epitaxy-level structures ever investigated in our spectroscopy focused laboratories.

### B. Experimental details

For photoluminescence (PL) measurements, the samples were mounted in a Helium-flow cryostat. Continuous wave (cw) PL was measured using the 325 nm emission line of a

a)Electronic mail: felix@physik.tu-berlin.de

HeCd laser. Resonant, high excitation PL, and time-resolved PL (TRPL) were performed using a XeCl laser pumped dye laser operating with 2-Methyl-5-t-Butyl-p-Quarterphenyl (DMQ) tuned to 370 nm. The pulse duration of this system amounts to 10 ns with a repetition rate of 100 Hz. To access shorter time scales, a frequency-doubled Ti:Sa laser, also tunable around 370 nm, with pulse durations of 2 ps, and a repetition rate of 5 MHz was used. Photoluminescence excitation (PLE) spectra were excited with a monochromatized 500 W Xenon arc lamp. The luminescence signal was dispersed by a SPEX 1404 additive double monochromator (PL, TRPL), a SPEX 1702 single monochromator (PLE), or a McPherson 2035 subtractive double monochromator (TRPL), whereas the detection was achieved with either a Hamamatsu multi-channel plate photomultiplier (S20 cathode) detector (TRPL), a bi-alkali photomultiplier (TRPL, PL), or a Princeton Instruments charge coupled device (PLE). The structural properties of the samples were studied by a Titan scanning transmission electron microscope made by FEI (Field Emission Inc.) operated at 300 kV with a semi-convergence angle of 9.0 mrad using a high angle annular dark field detector (STEM-HAADF) for Z-contrast imaging.

## III. RESULTS

Fig. 1 shows a low temperature PL spectrum of a quasi-SQW, that is non-resonantly excited at a moderate excitation power density of 5 $Wcm^{-2}$ (black, dashed line). A sharp emission peak of the QW ground-state transition is observed at an energy of around 2.44 eV. Repeating the same measurement under a much higher, resonant excitation with a power density of 5 $MWcm^{-2}$ (black, solid line) reveals two effects. First, the QW ground-state transition shifts by around 20 meV towards higher energies indicating a commonly reported weak QCSE.[4–8] At the same time, a significant broadening and an apparent asymmetry of the emission band are observed, which indicates band-filling.[20,21] Second, an additional, broad peak is observed at much higher energies, which we call the Confined Hole Continuum (CHC) luminescence. This particular luminescence is not associated with any distinct excitation channel as the photoluminescence excitation (PLE) spectrum from Fig. 1 (blue dashed line) shows. Even though this PLE measurement was performed at low excitation power densities, the same result is obtained when the measurement is repeated at elevated excitation power densities with a dye laser (not shown). Fig. 2 illustrates PL spectra of the same quasi-SQW (top) and a MQW-LED (bottom) obtained under comparable, resonant excitation conditions as a function of excitation power density. The CHC luminescence significantly broadens towards higher emission energies with increasing excitation density for both specimens, and no appearance of any distinct, well-resolved PL feature can be observed. While the CHC luminescence shown in Figs. 1 and 2 (top) is still mimicking a separate luminescence band at high excitation power densities, its true continuous evolution towards higher energies with rising excitation power becomes straightforwardly apparent in Fig. 2 (bottom). Owing to the vastly different time scales of the luminescence decays (later on introduced in Fig. 4) and the large temporal separation of the excitation pulses (10 ms), one always simultaneously records luminescence that corresponds to an entire range of

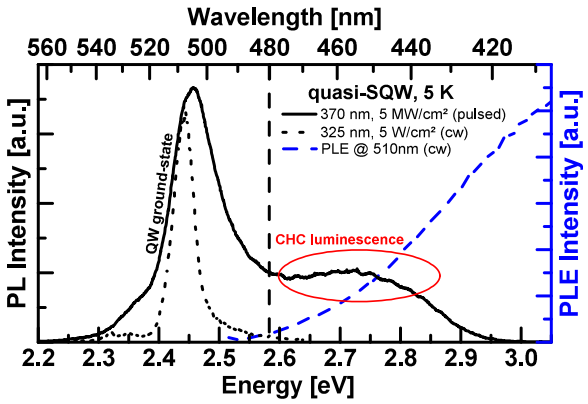


FIG. 1. Low temperature (5 K) photoluminescence spectra of a quasi-SQW, excited either non-resonantly (325 nm) with a HeCd laser (dashed, black line) or resonantly (370 nm) with a pulsed dye laser (solid, black line). A slight blue shift and a broadening of the emission peak towards higher energies (band-filling) are observed along with the drastically increased excitation power density. In addition, a broad luminescence band (the Confined Hole Continuum (CHC) luminescence) centered at around 2.75 eV is witnessed. The blue dashed line depicts a photoluminescence excitation spectrum with the detection centered at 510 nm. Here, no distinct excitation channels can be observed.

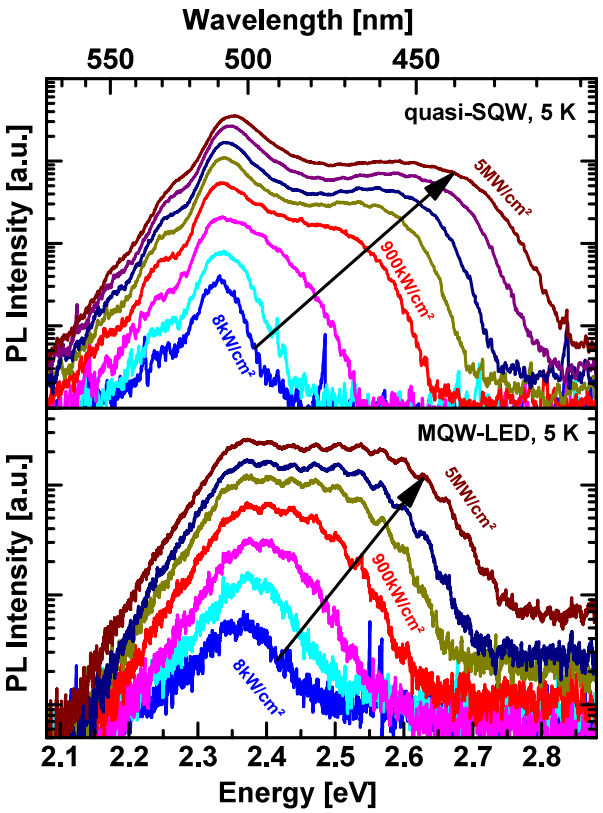


FIG. 2. Excitation power dependent series of low temperature (5 K) photoluminescence spectra comprising the same quasi-SQW depicted in Fig. 1 (top) and an additional MQW-LED (bottom). The highest excitation power density is equivalent to the black, solid line in Fig. 1. The broad CHC luminescence continuously shifts towards higher energies with rising excitation power density. The evolution of the spectra suggests a continuous density of states being involved in the overall luminescence process, well in agreement with the PLE results.

excitation conditions. This leads to a large variety of luminescence signatures, which all continuously broaden towards higher energies, but must not be misinterpreted as a separate luminescence band. Please note that at a first glance this particular behavior of the CHC luminescence resembles a Burstein-Moss shift as commonly observed in highly excited bulk material.[20,22] We note that the reported phenomenon can be easily distinguished from the dynamic processes characteristic for the QCSE. Fig. 3 shows the temporal evolution of the PL signal in response to an optical pulse. The top panel shows the results for a thin (2.2 nm) quasi-SQW sample, while the bottom panel presents the same measurement for a thick (4 nm) quasi-SQW. In both cases, two dynamic regimes can be observed. At low delay times, the CHC luminescence described above can be observed, whose dynamics will be analyzed in detail below. At large time delays, the de-screening of the QCSE is visible with a characteristic shift to lower emission energies over time as the internal fields are reestablished. Naturally, the QCSE is much more pronounced in the thick quasi-SQW sample (bottom panel), motivating our focus on thin QW samples (top panel) for an analysis of the CHC luminescence. In addition, a similar, continuous trend is also observed in TRPL measurements. We have measured the temporal decay of several samples at cryogenic and room temperature over a broad range of detection energies comprising the QW ground-state transition and the CHC luminescence. All decays are mono-exponential[23] and the corresponding decay times that result from a deconvolution with the instrument response function[24] are plotted in Fig. 4 (red squares) as a function of detection energy. Here, the decay times decrease drastically towards high energies in a *continuous* manner, in accordance with the *continuous* evolution of the CHC luminescence, cf. Fig. 2. In addition, the time-resolution of our setup permits the extraction of rise times (green circles in Fig. 4) as soon as the frequency-doubled Ti:Sa excitation can be applied (please see Section II for details). Again these time constants evolve in a similar way, i.e., they drastically and *continuously* decrease towards higher energies. In-line with PLE and PL results, the entire set of experimental trends shows no evidence for any kind of discrete state associated with the CHC luminescence. Fig. 5 introduces differential electroluminescence (EL) spectra of a MQW-LED sample. We obtain such differential spectra by optically pumping the sample into the optimal excitation regime for the CHC luminescence, cf. Fig. 2 (bottom). Simultaneously we apply an electrical bias to the LED structure and acquire the total luminescence signal. The spectra from Fig. 5 finally depict the differences of spectra obtained either with or without an applied bias. Naturally, one can clearly observe an EL peak belonging to the QW ground-state transition once the LED is operating in above threshold conditions (green line). As the optical excitation pulses are temporarily well separated, this EL is mostly generated in between the optical excitation events. Nevertheless, the main observation of Fig. 5 is related to the high energy tail of the differential spectra. Here, it is clearly shown that the CHC luminescence is not at all affected by the applied bias proving that the contributing carriers are still

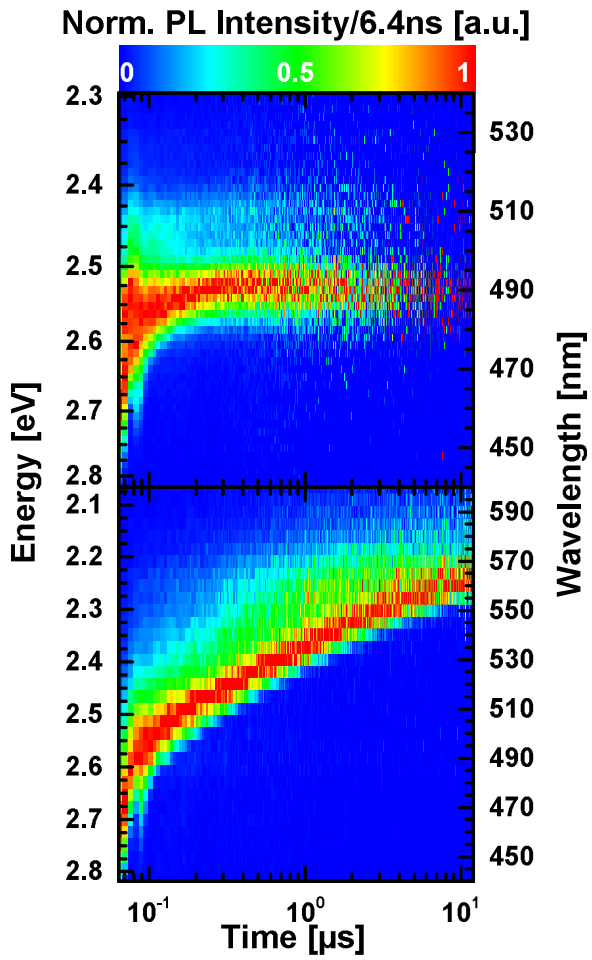


FIG. 3. Photoluminescence spectra as a function of delay time after excitation for a thin (2.2 nm, top) and thick (4 nm, bottom) specimen. The CHC luminescence at higher energies is observed to decay quickly, followed by a prolonged shift of the ground state luminescence due to de-screening of the QCSE. The latter is much more pronounced in the thicker sample.

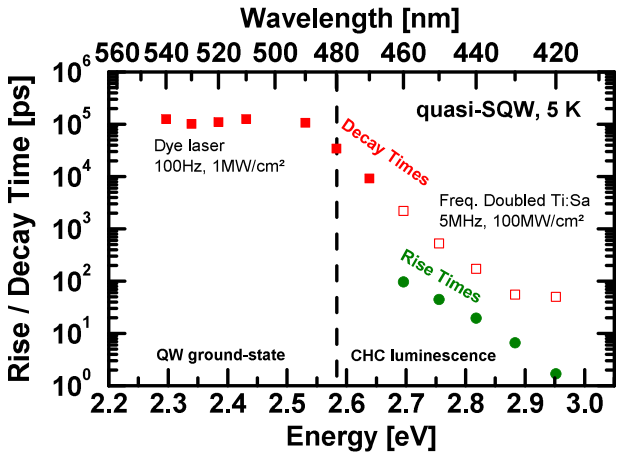


FIG. 4. Decay times (red squares) extracted from the mono-exponential decays observed at 5 K in a quasi-SQW. The filled, red squares correspond to excitation conditions as mentioned in the caption of Fig. 1, while the open, red squares were obtained with a frequency-doubled Ti:Sa laser, which also allowed the determination of the corresponding rise times (green circles). Please note the continuous evolution of the rise and decay times with rising detection energy that encompasses the luminescence of the QW ground-state and the CHC luminescence.

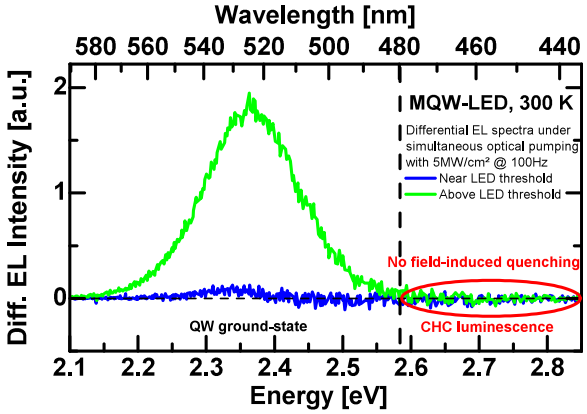


FIG. 5. Differential electroluminescence (EL) spectra of a MQW-LED sample, which is optically pumped similar to conditions shown in Fig. 2. Once the current flow is established, an EL peak is visible, originating from long times in between the optical excitation pulses. However, during the optical pulse, i.e., when the Confined Hole Continuum (CHC) luminescence is observed in photoluminescence, no effect of the applied bias on the CHC luminescence is observed, approving the confined nature of the CHC states. Please see the text for further details.

well confined despite the continuous nature of the CHC luminescence.

To exclude parasitic effects, we have also investigated a variety of control samples with focus on the CHC luminescence. A sample exclusively containing GaN barrier material in the active region (no InGaN QWs) showed no trace of any CHC luminescence. This excludes barrier, cap, or buffer GaN material as the source of the CHC luminescence. Series of QWs with differing indium compositions, QW thicknesses, and barrier doping concentrations as well as several production grade LED wafers have all shown the same luminescence characteristics described in Figs. 1–5. Interestingly, if the QW emission energy is tuned towards the blue spectral range (e.g., towards 450 nm), the overall effect of the CHC luminescence strongly diminishes. This observation can complementary be explained by an overlap of the QW ground-state and the CHC luminescence as well as an insufficient pump level. Here, in the blue spectral region, the reduced radiative lifetime of the QW ground state[23] must be counter-balanced by a drastic increase in excitation density, which naturally easily approaches excitation limitations governed by the samples' durability.

Subsequently, we can summarize the optical characteristics of the CHC luminescence as follows:

(i) The CHC luminescence is universally found in all high-quality samples we have investigated. We do not observe this intriguing optical signature in samples of limited structural quality or lower indium concentrations.
(ii) The CHC luminescence only occurs at high carrier densities, which are easily reached under resonant, pulsed optical excitation.
(iii) PLE spectra show no discrete excitation channel within the spectral range of the CHC luminescence. The absorption rather continuously increases towards the GaN band-edge. Power-dependent PL also shows a continuous broadening and a blue-shift of the high energy flank of the CHC luminescence.
(iv) Within the CHC luminescence, the decay and rise times of the PL signal decrease continuously and drastically with increasing emission energy.
(v) The CHC luminescence is robust against any temperature changes (not shown). It can be observed that both at cryogenic as well as room temperature and the decay as well as the rise times do not significantly scale with temperature.
(vi) The CHC luminescence is not suppressed for LEDs commonly applied bias values pointing towards carrier localization despite its continuous experimental signature. Hence, we observe the rare case of a well-confined state-continuum that contradicts commonly applied textbook perceptions of QWs.

## IV. DISCUSSION

Previous studies have attributed fast-decaying, high-energy shoulders[26] of InGaN QW emissions or even high energy peaks similar to the CHC luminescence[27] to in-plane, extended states, with main contributions arising from in-plane, localized QW states. In these models, such an in-plane localization arises from the potential minima created by In-rich regions in the QW. While this phenomenon can certainly describe high-energy shoulders with a certain ground-state separation, high-resolution transmission electron microscopy (HRTEM) measurements of our samples (see Fig. 6 for an example) preclude In-clusters and yield an In content of 19% with a completely random distribution of the In atoms.[25] Please note that a pronounced In-clustering would be required in order to explain localization over the entire spectral range of the CHC luminescence reaching up to 0.4 eV above the QW ground-state transition. In addition, such In-clustering would result in strong non-monotonicity

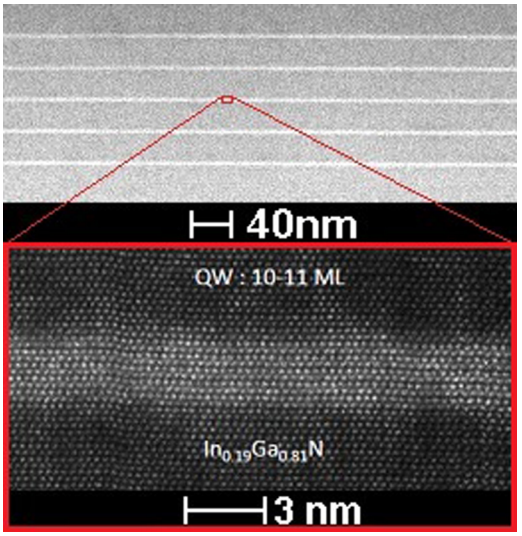


FIG. 6. Transmission electron micrographs of a typical quasi-SQW. The top panel shows an overview while the bottom panel depicts a high-resolution detail of one of the quantum wells. We observe abrupt InGaN/GaN interfaces and no thickness variations beyond a single monolayer. There is no evidence of phase separation in the InGaN quantum wells nor any composition fluctuations beyond the random distribution of In atoms.[25] Therefore, the optical properties of such a QW sample will not be dominated by any In-induced potential fluctuations.

of the observed transient decays. Also, we can exclude V-Pits[28,29] as the source of the CHC luminescence. Extensive micro-PL mapscans with a spatial resolution of around 300 nm (Ref. 30) did not reveal any luminescence traces of the thinner QWs on the facets of V-Pits. Such luminescence contribution would appear as energetically sharp lines with a spot-like lateral distribution.[28] In addition, the well-known S-shape that can be observed in temperature-dependent PL measurements as a signature of in-plane localization[31] due to Indium fluctuations[10] is limited to less than 10 meV in all our samples (or does not exist at all in the case of thicker QWs). We can therefore also exclude any in-plane localization as the source of the CHC luminescence due to its large energetic separation from the QW ground-state transition. In order to coherently explain all our observations, we propose the model sketched in Fig. 7. As soon as the active region is highly pumped, the hole ground-states are increasingly saturated. The absorption below the GaN band edge, however, still allows the creation of electron-hole pairs, consisting, for example, of ground-state electrons and highly excited holes. Naturally, these holes can still relax towards the QW. However, due to Pauli-blocking, this cascade ends in excited hole states (solid violet in Fig. 7) which lie energetically below the confinement potential of the QW, but still above the GaN band edge. These states are bulk-like, as they derive from GaN bulk valence band states in the adjacent barrier. Nevertheless, these states are still confined due to the tilted valence band edge in the barriers arising from polarization field discontinuities. Hence, in the depicted model, the holes are to some extent delocalized in the out-of-plane direction of the QW. Thereby the described model is consistent with all the characteristics of the CHC luminescence (i–vi). In particular, this means:

(I) The CHC luminescence will arise regardless of the precise properties of the individual InGaN QW. It is a general feature of InGaN/GaN heterostructures that the band offset in the valence band[32] is smaller in regard to the energetic difference between the excited and ground electron states. This general property enables hole states forming a quasi-continuum that protrudes out of the QW and is significantly populated well before all electron states within the QW are filled. We note that, in principal, the same quasi-continuum of states exists for electrons above the confined excited electron states. In contrast to the CHC states, these are not accessible by our excitation conditions, because the energetic difference between this Confined Electron Continuum and the hole ground states is larger than the energy of the pump photons.

(II) The high energy CHC luminescence can only be observed once the ground hole states as well as all truly confined excited hole states have been filled. Due to inhomogeneous broadening of the ground state transition and due to the energetic proximity of the ground and excited hole states, a direct observation of the excited hole state recombinations as distinct features in the spectrum is not possible. Therefore, high excitation power densities and superior crystal quality are necessary to saturate the hole states in the QW, allowing the observation of the CHC luminescence. We wish to remark that exactly this high excitation regime constitutes the basis for any high power LD applications, especially in the green spectral range.

(III) Because of the continuous hole state density originating from the bulk GaN-like hole states of the CHC luminescence, it is not surprising that the absorption and emission characteristics scale rather continuously upon variation of the excitation conditions as well. The excited electron state, marked with a dotted, red line in Fig. 7 may play a role as well at even further elevated excitation powers or under non-resonant pumping conditions, but all presented spectra are still dominated by the CHC states. Please note that any further contribution of excited electron states should show up as discrete luminescence features,[33] however, any overlap with the CHC luminescence may spoil this observation.

(IV) The rise times of the time-resolved photoluminescence decay can be attributed to the relaxation time of the excited holes. The corresponding values decrease towards higher emission energies, as the holes (excited into the bulk-like state continuum below the QW confinement potential) need to interact with a diminishing number of acoustic phonons in order to reach their final CHC states. The drastically reduced decay times across the CHC luminescence are related to the higher wave function overlap between the ground-state electrons (solid red line in Fig. 7) and the excited out-of-plane delocalized hole states (violet color gradient in Fig. 7) in contrast to the hole ground-states, which suffer from the QCSE (green line).

(V) As soon as the excited hole-states become less localized within the QW, they are more prone to interact

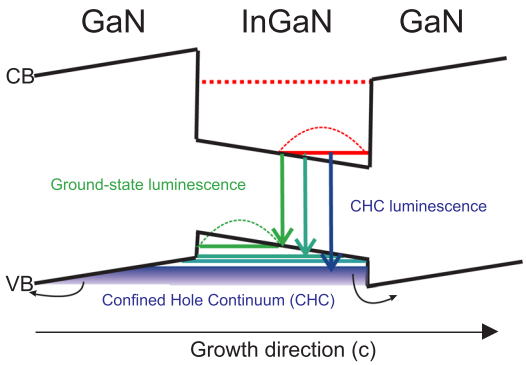


FIG. 7. Sketch of the proposed model for the observed Confined Hole Continuum (CHC) luminescence. Under high optical pumping, the hole ground-states (green line) are saturated and excited hole-states (cyan lines) are populated. Once all discrete hole-states are filled, additional quasi-continuous hole-states below the GaN valence band edge (violet color gradient) are populated. These CHC states, despite their continuous nature, are still confined by the triangular potential arising from the internal polarization fields. Hence, the CHC states are more extended along the c-direction if compared to the ground and still confined excited states.

with point defects (at the InGaN-GaN interfaces or in the GaN barrier layers). In addition, the energy that is needed to overcome the remaining potential barrier is small enabling hole leakage under high excitation conditions (see curved black arrows in Fig. 7). The lack of a pronounced temperature dependence of the CHC luminescence's decay times suggests that the decay is still dominated by non-radiative processes at cryogenic temperatures.

(VI) The fact that the CHC luminescence does not diminish when a bias is applied to the sample proves that the holes involved are still sufficiently confined by the triangular potential, as otherwise they would be extracted from the active region, recombine elsewhere, and thus reduce the observed intensity. Hence, as indicated in Fig. 7, the tilted band structure in the active region still provides a confinement potential for hole states, which would otherwise be completely delocalized similar to bulk GaN valence band states.

## V. CONCLUSION

The Confined Hole Continuum (CHC) luminescence that we universally observe in all green-emitting, high quality InGaN QWs is the signature of a so far frequently neglected loss mechanism arising under high pumping conditions. As soon as the confined hole states are saturated, all additional holes introduced into the system relax into out-of-plane less localized states. In such states, holes can interact with more non-radiative centers and the overall hole escape rate is enhanced. Obviously, this phenomenon hinders any high power applications. Finally, we suggest two solutions in order to overcome the issue associated with the CHC luminescence:

(A) The use of AlGaN barriers instead of GaN barriers would increase the valence band offset and shift the CHC luminescence to higher energies, while simultaneously increasing the number of confined hole states.[34]

(B) The valence band offset can also be enlarged by incorporating higher amounts of indium into thinner QWs,[35] thus reducing the significance of CHC states.

Obviously, both of these solutions are technologically challenging and warrant further research. Additionally, we wish to note that the growth on non-polar planes cannot offer a solution for this particular challenge. Close to any flat-band conditions, the excited hole states would not be additionally confined by any triangular potential and hole leakage would be expected to be increased even further under high-pumping conditions. The increased electron-hole overlap in such non-polar structures, however, would help to reduce carrier lifetime and hence shift the excitation powers necessary to saturate the QW states to higher excitation power densities.

In conclusion, we have identified a commonly neglected loss mechanism, which arises from a confined hole continuum (CHC). This loss occurs at high carrier densities constituting its importance for high power LEDs and LDs in the green spectral region.

## ACKNOWLEDGMENTS

We gratefully acknowledge the financial support of the European Union FP7-ICT Project NEWLED, No. FP7-318388 and the German Science Foundation within the Collaborative Research Center (CRC 787).

[1]S. Nakamura, M. Senoh, N. Iwasa, and S. Nagahama, Jpn. J. Appl. Phys. **34**, L797 (1995).
[2]Y. Narukawa, J. Narita, T. Sakamoto, K. Deguchi, T. Yamada, and T. Mukai, Jpn. J. Appl. Phys. **45**, L1084 (2006).
[3]M. R. Krames, O. B. Shchekin, R. Mueller-Mach, G. O. Mueller, L. Zhou, G. Harbers, and M. G. Craford, J. Disp. Technol. **3**, 160 (2007).
[4]J. Seo Im, H. Kollmer, J. Off, A. Sohmer, F. Scholz, and A. Hangleiter, Phys. Rev. B **57**, R9435 (1998).
[5]L.-H. Peng, C.-W. Chuang, and L.-H. Lou, Appl. Phys. Lett. **74**, 795 (1999).
[6]F. Della Sala, A. Di Carlo, P. Lugli, F. Bernardini, V. Fiorentini, R. Scholz, and J.-M. Jancu, Appl. Phys. Lett. **74**, 2002 (1999).
[7]J. Bai, T. Wang, and S. Sakai, J. Appl. Phys. **88**, 4729 (2000).
[8]T. Wang, J. Bai, S. Sakai, and J. K. Ho, Appl. Phys. Lett. **78**, 2617 (2001).
[9]Y. Narukawa, Y. Kawakami, S. Fujita, S. Fujita, and S. Nakamura, Phys. Rev. B **55**, R1938 (1997).
[10]S. Chichibu and A. Abare, Appl. Phys. Lett. **73**, 2006 (1998).
[11]N. Duxbury and U. Bangert, Appl. Phys. Lett. **76**, 1600 (2000).
[12]P. Ruterana and S. Kret, J. Appl. Phys. **91**, 8979 (2002).
[13]H. K. Cho, J. Y. Lee, J. H. Song, P. W. Yu, G. M. Yang, and C. S. Kim, J. Appl. Phys. **91**, 1104 (2002).
[14]Y.-H. Cho, S. K. Lee, H. S. Kwack, J. Y. Kim, K. S. Lim, H. M. Kim, T. W. Kang, S. N. Lee, M. S. Seon, O. H. Nam, and Y. J. Park, Appl. Phys. Lett. **83**, 2578 (2003).
[15]J. Jinschek, R. Erni, N. Gardner, A. Y. Kim, and C. Kisielowski, Solid State Commun. **137**, 230 (2006).
[16]A. Laubsch, M. Sabathil, W. Bergbauer, M. Strassburg, H. Lugauer, M. Peter, S. Lutgen, N. Linder, K. Streubel, J. Hader, J. V. Moloney, B. Pasenow, and S. W. Koch, Phys. Status Solidi C **6**, S913 (2009).
[17]M. Binder, A. Nirschl, R. Zeisel, T. Hager, H.-J. Lugauer, M. Sabathil, D. Bougeard, J. Wagner, and B. Galler, Appl. Phys. Lett. **103**, 071108 (2013).
[18]J. Iveland, L. Martinelli, J. Peretti, J. S. Speck, and C. Weisbuch, Phys. Rev. Lett. **110**, 177406 (2013).
[19]F. Nippert, S. Karpov, I. Pietzonka, B. Galler, A. Wilm, T. Kure, C. Nenstiel, G. Callsen, M. Straßburg, H.-J. Lugauer, and A. Hoffmann, Jpn. J. Appl. Phys. **55**, 05FJ01 (2016).
[20]E. Burstein, Phys. Rev. **93**, 632 (1954).
[21]H. C. Casey, J. Muth, S. Krishnankutty, and J. M. Zavada, Appl. Phys. Lett. **68**, 2867 (1996).
[22]B. E. Sernelius, K.-F. Berggren, Z.-C. Jin, I. Hamberg, and C. G. Granqvist, Phys. Rev. B **37**, 10244 (1988).
[23]P. Lefebvre, A. Morel, M. Gallart, T. Taliercio, J. Allegre, B. Gil, H. Mathieu, B. Damilano, N. Grandjean, and J. Massies, Appl. Phys. Lett. **78**, 1252 (2001).
[24]D. V. O'Connor, W. R. Ware, and J. C. Andre, J. Phys. Chem. **83**, 1333 (1979).
[25]T. Schulz, T. Remmele, T. Markurt, M. Korytov, and M. Albrecht, J. Appl. Phys. **112**, 033106 (2012).
[26]M. J. Davies, T. J. Badcock, P. Dawson, M. J. Kappers, R. A. Oliver, and C. J. Humphreys, Appl. Phys. Lett. **102**, 022106 (2013).
[27]G. Sun, G. Xu, J. Yujie, H. Thao, G. Liu, J. Zhang, and N. Tansu, Appl. Phys. Lett. **99**, 081104 (2011).
[28]A. Hangleiter, F. Hitzel, C. Netzel, D. Fuhrmann, U. Rossow, G. Ade, and P. Hinze, Phys. Rev. Lett. **95**, 127402 (2005).
[29]T. L. Song, J. Appl. Phys. **98**, 084906 (2005).
[30]J. S. Reparaz, G. Callsen, M. R. Wagner, F. Güell, J. R. Morante, C. M. Sotomayor Torres, and A. Hoffmann, APL Mater. **1**, 012103 (2013).
[31]Y.-H. Cho, G. H. Gainer, A. J. Fischer, J. J. Song, S. Keller, U. K. Mishra, and S. P. DenBaars, Appl. Phys. Lett. **73**, 1370 (1998).
[32]P. G. Moses and C. G. Van de Walle, Appl. Phys. Lett. **96**, 021908 (2010).
[33]T. Schulz, A. Nirschl, P. Drechsel, F. Nippert, T. Markurt, M. Albrecht, and A. Hoffmann, Appl. Phys. Lett. **105**, 181109 (2014).
[34]Y.-D. Lin, S. Yamamoto, C.-Y. Huang, C.-L. Hsiung, F. Wu, K. Fujito, H. Ohta, J. S. Speck, S. P. DenBaars, and S. Nakamura, Appl. Phys. Express **3**, 82001 (2010).
[35]S.-M. Ko, H.-S. Kwack, C. Park, Y.-S. Yoo, S.-Y. Kwon, H. Jin Kim, E. Yoon, L. Si Dang, and Y.-H. Cho, Appl. Phys. Lett. **103**, 222104 (2013).